SEISMIC BEHAVIOR OF LOW-YIELD DOUBLE STEEL PLATE AND CONCRETE SHEAR WALLS

Chin-Tung CHENG[1], Jhe-Li SU[2], Yi-Shan LIN[3], Chau-Cho YU[4] and Chi-Ming LAI[5]

SUMMARY

In this research, low-yield double steel plate concrete shear wall is consisted of two steel faceplates with concrete infill connected by shear connector. In the early research and development, it was mostly used in ice-resisting platform, nuclear power plants and ship hulls to resist in-plane or out-plane forces and increase its stiffness simultaneously. Recent research focuses on its application in high-rise buildings. Since Taiwan is located in high seismic region, effect of near-fault dynamic loads with high strain rate needs to be clarified. Four specimens were constructed and tested in NCREE Tainan Laboratory, having the same aspect ratio of 1.0 and thicknesses. The steel faceplate of the specimens was made of low-yield steel with high ductility properties. It can lower its shear strength to reduce the amount of shear studs used in inner wall. The primary investigate parameter includes seismic effect of flange wall to the shear wall and strain rate of applying loads in static, high strain rate load or shaking table tests, respectively. Based on test results, the dynamic loads with high strain rate will increase the ultimate strength and displacement of composite walls, resulted in a better energy dissipation capacity of the specimens.

***Keywords**: Low-Yield Steel, Double Steel Plate, Composite Shear Wall, In Plane Cyclic Loading, Reinforcement Ratio, Axial Load Ratio, Slenderness Ratio, Shaking Table Test.*

INTRODUCTION

Concrete-filled double-skin composite walls (CDCWs) have been used in the ice-resisting platform for Arctic offshore structures (Ohno et. al. 1987, Matsuishi and Iwata, 1987), ship hulls (Huang et al. 2014), nuclear power plants (Fukumoto et al. 1987, Ozaki et al. 2004, Rahai and Hatami, 2009, Vecchio and McQuade, 2011, Danay, 2012, Varma, 2014, Epackachi et al. 2015, Seo et al. 2016, Kurt et al. 2016, and Yan and Liew, 2016), and shear walls in buildings (Eom et al. 2009, Hu et al., 2014, Nie et al. 2013, Nie et al. 2014, Chen et al. 2015 and Zhao et al. 2016). Experimental investigation in literatures showed that CDCWs exhibited excellent lateral strength and deformation capacity. CDCWs consist of structural steel modules that are filled with plain or high strength concrete to develop composite systems. As shown in Fig. 1 (Epackachi et al. 2015a), the steel modules are composed of (i) two steel faceplates that form the surfaces of the CDCWs, (ii) uniformly distributed shear studs in the inner walls of steel faceplates, and (iii) tie bars or rods connecting the two faceplates together (Seo et al. 2016) . The shear studs provide composite action for steel faceplates and concrete infill, and the tie bars fasten two steel faceplates serving as formwork for the pouring of concrete infill. The steel modules can be fabricated

[1] *Professor, Department of Constructional Engineering, National Kaohsiung University of Science and Technology, Taiwan, e-mail: ctcheng@nkust.edu.tw*
[2] *Master Student, Institute of Department of Civil and Environmental Engineering, National University of Kaohsiung, Taiwan, e-mail: m1095208@mail.nku.eud.tw*
[3] *Mater student, Department of Civil Engineering, National Cheng-Kung University, Taiwan, Email:n66104068@mail.ncku.edu.tw*
[4] *Associate Professor, Institute of Department of Civil and Environmental Engineering, National University of Kaohsiung Taiwan, e-mail: ccyu@nku.edu.tw*
[5] *Professor, Department of Civil Engineering, National Cheng-Kung University, Taiwan, e-mail: cmlai@mail ncku.edu.tw*

in shops with quality control, and shipped to the site for the assembly of construction. CDCWs can improve the construction efficiency and cost-saving over conventional reinforced concrete (RC) construction.

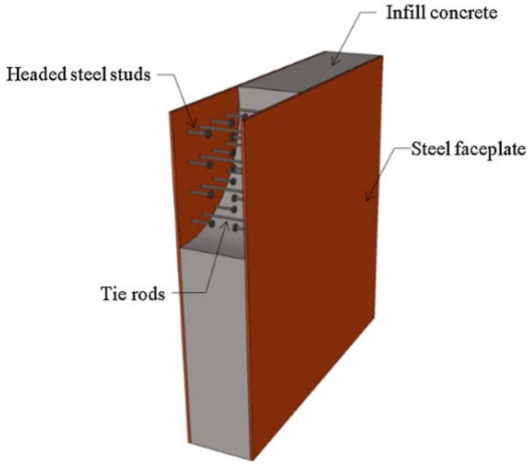

Fig. 1 Typical cross section of concrete filled steel plate shear walls (Epackachi et al. 2015a)

Experimental studies have been conducted in Japan, S. Korea, Mainland China, and the US to investigate the in-plane shear behavior of CDCWs. These researches have focused on the pure in-plane shear behavior of CDCW panels which may be used in commercial building construction and safety-related nuclear facilities. To avoid the welding failure of steel faceplates at the base, all specimens in literatures were embedded in a concrete foundation and loaded at the top of specimens in a cantilever way, resulting in a large moment demand at the specimen base. Therefore, the behavior of CDCWs without the support of boundary elements is governed by the flexure failure at the base due to the crushing of concrete and buckling of steel faceplates, and shear failure does not occur for wall aspect ratios greater than or equal to 0.60 (Seo et al. 2016). In this paper, wall specimen ends are surrounded by boundary plates and tested by a new setup that deforms the specimen in a double curvature. The specimens may be failed due to shear yielding of steel faceplate rather than literature's flexural buckling, benefited from the decrease of the flexural moment demand at top and bottom wall boundary.

Low-yield steel has the advantage of extending the ductility of steel faceplate and reducing the amount of shear studs used in inner walls of steel faceplate. However, it is not gained enough attention in the application of low-yield steel on composite walls. Besides, it is important to clarify the effect of higher axial load on the seismic behavior of composite walls before its application in high rise-buildings. In the research of Ji et al. 2017, experimental and analytical investigation indicated that axial compression has limited influence on the shear strength, but decreases the shear-deformation capacity of the composite walls. The high axial load may potentially lead to the crushing of concrete infill prior to the yielding of the steel faceplate. In addition, effect of near-fault dynamic load with high strain rate is another parameters needs to investigate, when structures locate in high seismic region.

Therefore, the objective of this research is to investigate in-plane shear performance of concrete-filled low-yield-steel-plate composite walls in high-rise buildings at high seismic region. To validate the proposed idea, four reduced-scale composite walls were constructed and tested by a new established test setup at Tainan Lab. National Center for Earthquake Engineering (NCREE) in Taiwan. The primary investigate parameter includes seismic effect of flange to the shear wall and strain rate of applying loads in static, high strain rate load or shaking table tests, respectively. Seismic response of structures varied with investigating parameters is evaluated.

EXPERIMENTAL PROGRAMS

As shown in Fig. 2, all specimens have aspect ratio of 1.0, having the dimension of 1200X1200X106 mm in size that is reduced approximately 2.5 times from a prototype structure with story height 3000 mm and wall thickness of 250 mm, respectively. Table 1 shows the specimen design and investigated parameters. The reinforcement ratio of composite walls in safety-related nuclear facilities is ranging 1.5-5% with head to head shear studs in inner shear walls as shown in Fig. 1. In this paper, two 8 mm thick low-yield steel faceplates sandwiched 10 cm thick concrete infill and connected by interlaced shear studs, having 13.8% reinforcement ratio, as shown in Fig. 3. Since the shear studs were interlaced, the reinforcement ratio in this paper should be divided by two, when

compared with head to head shear studs as shown in Fig.1. The slenderness ratio of steel faceplate is 25 for specimens with 20 cm spacing of shear studs in inner walls divided by 0.8 cm thick steel faceplate. This ratio is far less than required slenderness ratio of 44.7, which is calculated on the basis of the research by Zhang et al. 2014 as

$$\frac{S}{T_p} = \sqrt{\frac{E_s}{F_y}} \quad (1)$$

where S is the spacing of shear studs or bolts, and E_s and F_y elastic modulus and yield strength for steel faceplates, respectively. For specimens with 20 cm spacing of shear studs, the required slenderness ratio of 31.6 is calculated by replacing yield strength Fy (100 MPa) of steel faceplate with tensile strength Fu=200MPa in equation (1). The tensile strength Fu is obtained from stress-strain curve of low-yield steel by a target drift ratio 4% that the wall may experience under extreme loads. For a conservative purpose with higher axial load applied on tested specimen, the required slenderness ratio 31.6 is further decreased by multiplying 0.8, based on test results of Cheng et.al. 2019.

Figure 3 shows the shear studs arrangement in inner wall of specimens with studs spacing of 20 cm. In which, upper figure also show 9-100 mm diameter steel tubes inserted on the shear wall for the specimens LNL-F20 and LNL-FEQ, which have flange wall on both ends of the shear wall. While 16-100 mm diameter steel tubes inserted on the shear wall for the specimens LNL-20 and LNL-EQ without flange wall. The dimension of flange wall is 250 mm wide and 100 mm thick on each side of the shear wall. There are 50 mm gap between the flange wall and top base plate so that axial load was applied on the shear wall only as shown in Figure 2. As shown in lower figure of Fig. 3, flange walls with dimension of 200 mm wide and 100 mm thick on each side of shear wall were not welded to the shear wall. The presence of the tube is trying to reduce stiffness and strength of the shear wall. The objective of the flange wall is acting as a lateral support for shear wall in shaking table tests.

In literature, test specimens were embedded in a concrete foundation to avoid the welding failure of steel faceplates at the base. Without the support of boundary elements, the behavior of CDCWs is governed by the flexure failure at the base due to the crushing of concrete and buckling of steel faceplates. In this paper, to mitigate the concrete crushing during tests, a 10 mm steel plate acted as boundary element for composite walls was applied to protect the concrete infill from crushing, and wall specimens were installed to the test machine through top and bottom base steel plates. In all interfaces, full penetration welds were applied to connect walls to the base plates and wall boundary. To avoid the welding failure at the interface, stiffener plates were used as shown in Fig. 2. Table 2 shows the material strength for the steel. The concrete was poured from the holes at the top base plate. The concrete strength at the test day was 42.3 MPa for the first two specimens; while it was 53.8 MPa for the last two specimens as shown in Table 1.

Table 1 Investigated parameters of design specimens

Specimen	Axial load ratio (P/Pu)	Shear strain rate (rad/s)	Thickness of whole wall T (cm)	Thickness of faceplate T_P (cm)	Reinforcement ratio T_P /T (%)	Spacing of shear studs S (cm)	Design slenderness ratio (S/T_P)	Required slenderness ratio (S/T_P)
LNL-F20	0.09	0.003	11.6	0.8	13.8	20	25	25.3
LNL-FEQ		0.3						
LNL-20		0.003						
LNL-EQ		0.3						

Table 2 Material strength for the steel

Coupon test	Yield strength Fy (MPa)	Tensile strength Fu (MPa)
8 mm faceplate	108	272
10 mm boundary plate	273	426
25 mm top and bottom end plate	268	433

Investigated parameters includes seismic effect of flange of specimens and strain rate of applying loads with static, high strain rate load or shaking table tests, respectively. In test numbering, the first character, L, means the low-yield steel used as steel faceplate, while the second character, N, represents concrete thickness of 10 cm. And the third character, L, stands for low axial load ratio of 0.09 applied on tested specimens. The last group of number or character in 20 and F20, means specimens tested by static loading protocol, while EQ and FEQ tested by high strain rate earthquake-type loads. In which, the load of EQ and FEQ is applied by several earthquake waves with successive increasing intensity of accelerations, such as 0.05g, 0.1g, 0.15g, 0.2g and 0.25g, etc. As

shown in Fig. 4, all specimens were tested by biaxial test system (BATS) with successive in-plane shear and constant axial loads. The specimen was fixed at top base plate through high strength bolts and then applied with a constant axial load (530kN) by 30000 kN vertical actuators. Then, 4000 kN actuators at bottom base applied the static loading of cyclic reversed horizontal load with displacement control in the form of triangular waves as shown in Fig. 4. Fig. 5 shows the high strain rate dynamic loading applied with displacement control by a recorded wave from Chichi Earthquake with a shear strain rate of 0.3 rad/sec recommended by Lanning et al. 2016. Four transducers measured the displacement of specimens and monitored the slip in interfaces between the specimen and test facility. Before each test, strain rosettes and strain gauges were applied to monitor the strain development on the shear panel and boundary plates.

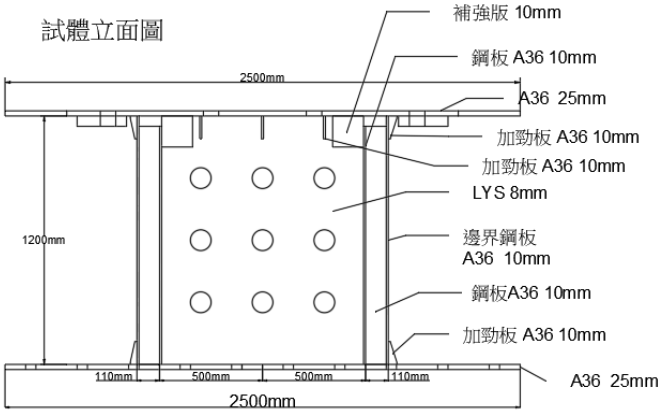

Fig. 2 Graph shows the appearance of composite walls with flange

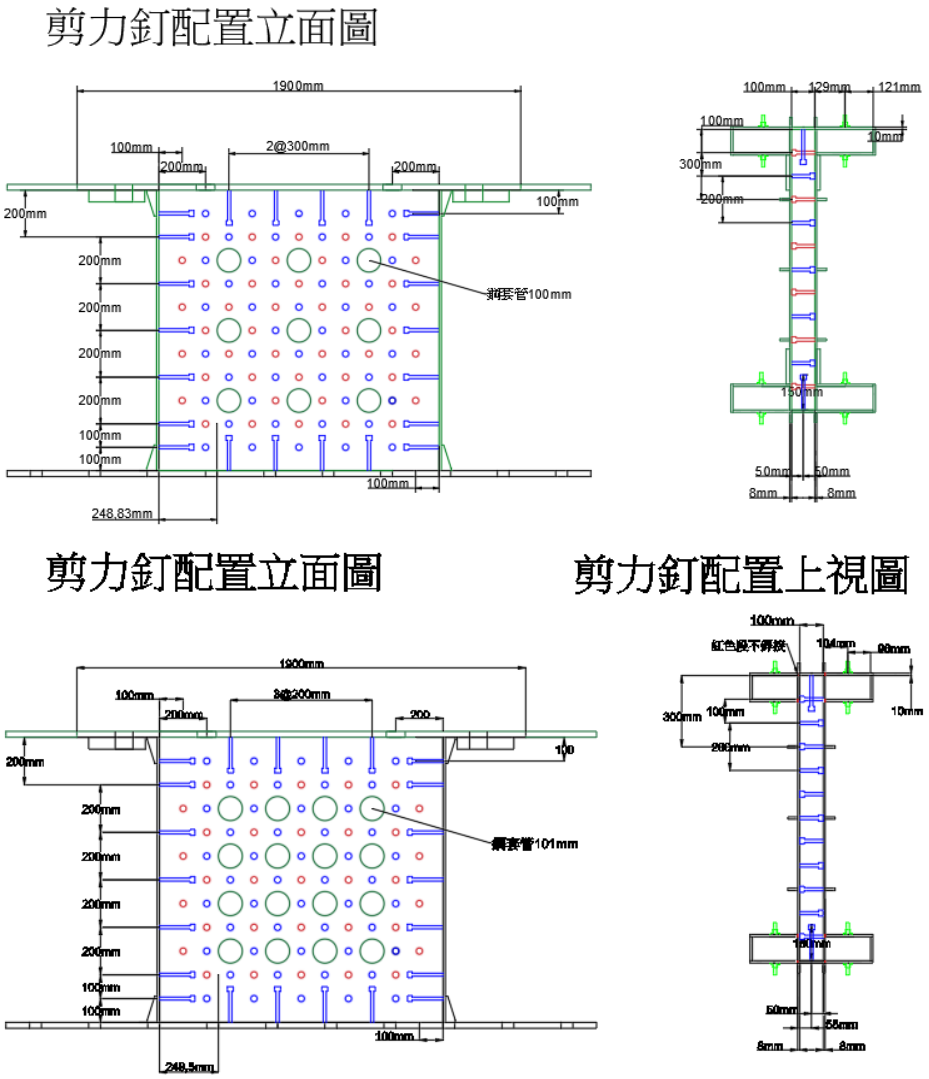

Fig 3 Graph shows the pattern of shear studs in inner wall for specimens with studs spacing of 20 cm

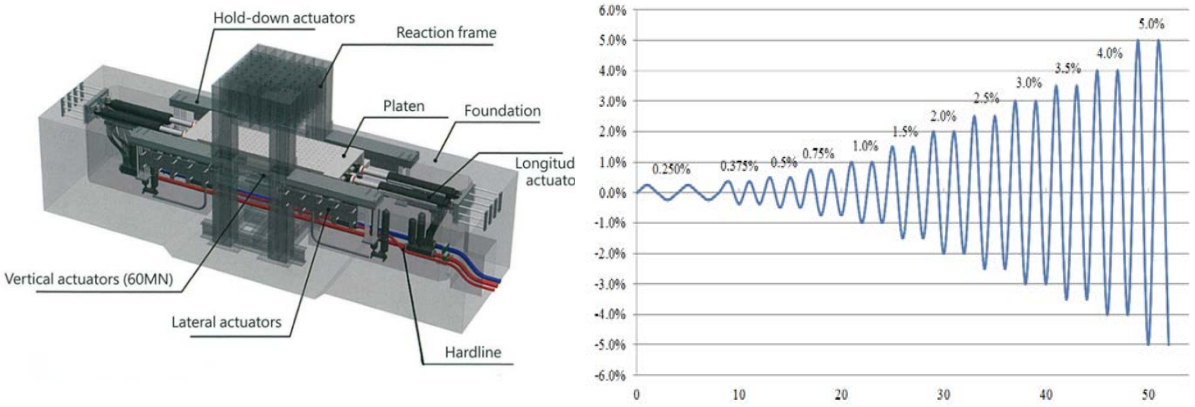

Fig. 4 Graphs respectively show the test facility (BATS) and static loading protocol

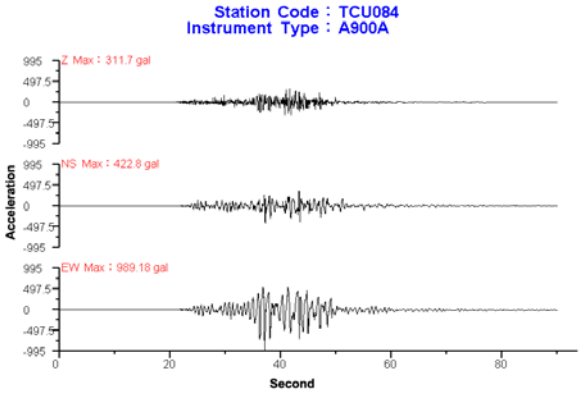

a) A record from Chichi Earthquake

Fig. 5 Graphs respectively show the dynamic loading protocols

Before the tests of LNL-EQ and LNL-FEQ, shaking table test was firstly conducted. Since the specimens behaved in an elastic manner throughout shaking table test, high strain rate dynamic tests were then performed to get extreme state damage of the walls. Fig. 6 shows the elevation view of the specimen and concrete mass in shaking table test, in which three concrete blocks totally weighted 54 tons. Three earthquake records such as El-Centro, Kobe and Chi-Chi TCU084 were applied in successive increasing intensity levels of acceleration. In the beginning and the end of tests, white-noise excitation with 0.1g intensity was applied to evaluate the vibrating frequency of the specimens.

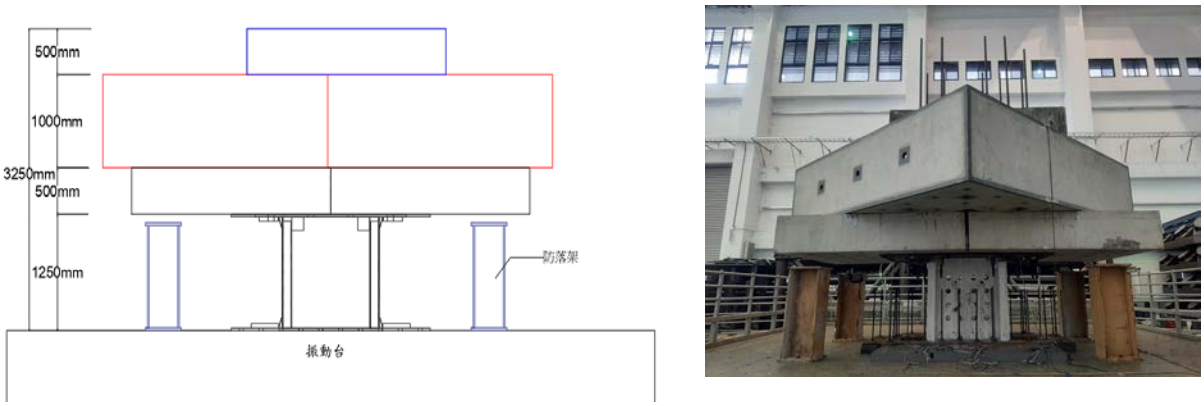

a) Side view b) Photo

Fig. 6 Graph and photo show the elevation view of specimen and concrete mass in shaking table test

TEST RESUTLS

In the test of LNL-F20, plaster paint on stiffener plate peeled off, welding crack on boundary plate developed near the tip of top stiffener plate, and diagonal global buckling of steel faceplate, successively occurred at the drift cycle of 2.0%, 4.0% and 5.0%, respectively. The lateral strength deteriorated and test terminated at the drift cycle of 6%, and 4% respectively for specimens LNL-F20 and LNL-20. At final loading stage, it is found that specimen LNL-F20 with flange wal failed due to diagonal global buckling of steel faceplate, while it is local buckling of steel faceplates near top and bottom base plates and welding fracture at top and bottom stiffener for the test of LNL-20 without flange wall due to the fastening of faceplates by 16 tubes on the wall. The damage sequence and failure mechanism for specimens subjected to high strain rate dynamic tests is similar to its corresponding static tests.

Fig. 7 shows the hysteretic curves for four specimens. Its detailed test results are summarized in Table 3, in which initial stiffness was calculated by shear strength corresponding to the drift of 0.1%, and the ultimate displacement was defined as the displacement when its lateral strength descending 85% from the peak strength. As shown in Fig. 7, all tests exhibited plump hysteretic curve, which shows very good energy dissipation of tested specimens. The ultimate displacement for all tests ranges 3.8 % to 7.5%. The presence of flange wall increases 22% (630 kN) and 19% (560kN) of the peak strength under static and high strain rate loads, respectively. As shown in Table 3, peak strength of high strain rate dynamic tests in LNL-EQ is averagely 5.6% larger than that of static test in LNL-20. Similarly, peak strength of high strain dynamic tests in LNL-FEQ is averagely 2.6% larger than that of static test in LNL-F20. As shown in Table 3, the ultimate displacement in high strain rate dynamic tests in LNL-FEQ and LNL-EQ is averagely 2% and 0.7% more than that of corresponding static tests, respectively. As results, energy dissipation capacity in high strain rate dynamic tests is found greater than that of static tests.

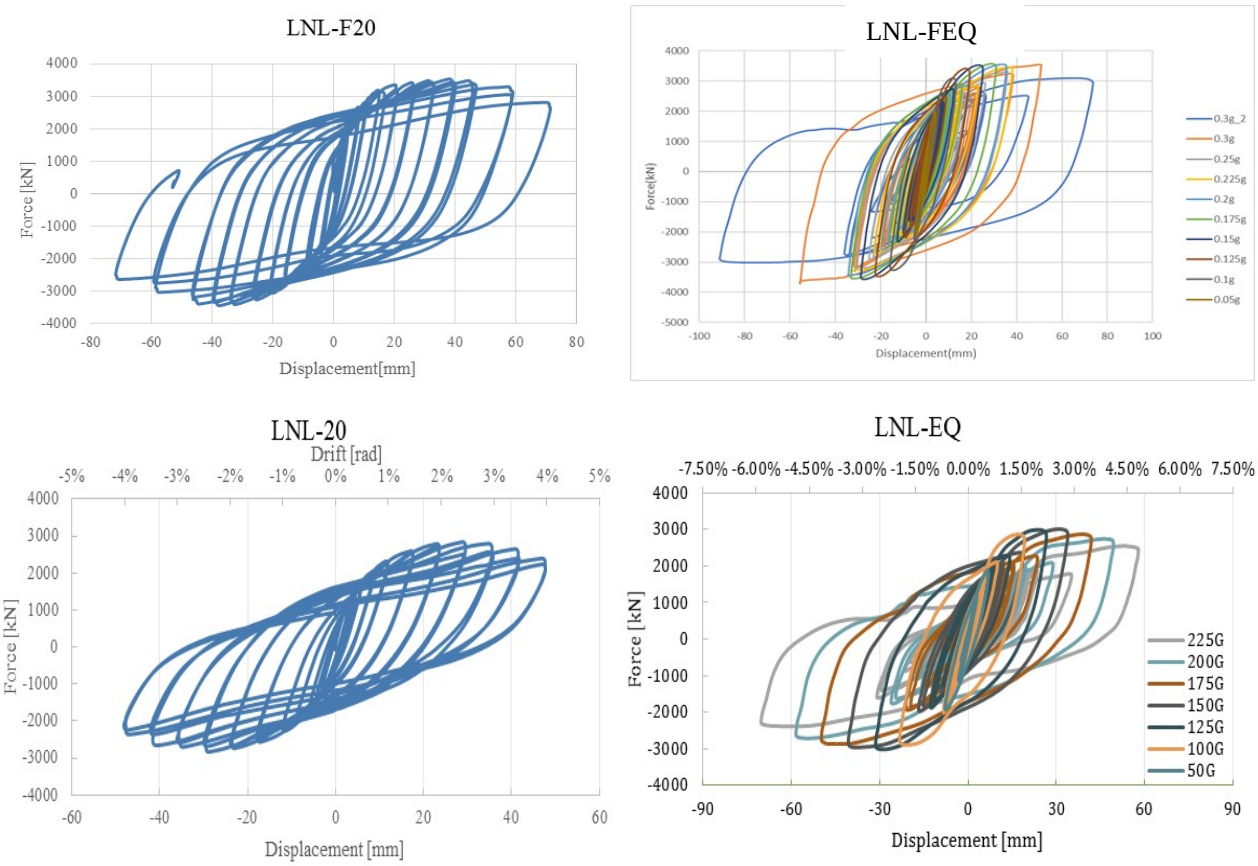

Fig. 7 Graphs show hysteretic curves for each specimen

Table 3 Summary of test results

Specimens	Initial Stiffness (kN/mm)	Yielding Strength		Peak Strength		Ultimate Displacement	Ductility
		Force (kN)	Δ_y(%)	Force (kN)	Δ_{max}(%)	Δ_u(%)	Δ_u / Δ_y
LNL-F20	1013	+1231/ -1306	+0.172/ -0.147	+3521/ -3449	+3.178/ -3.156	+4.815/ -4.871	28/ 33
LNL-FEQ	695	+1436/ -1240	+0.188/ -0.127	+3526/ -3622	+2.390/ -4.632	+6.144/ -7.585	33/ 60
LNL-20	511	+761/ -856	+0.128/ -0.097	+2849/ -2848	+2.416/ -2.394	+3.866/ -3.822	30/ 40
LNL-EQ	417	+865/ -821	+0.168/ -0.172	+3011/ -3017	+2.575/ -2.415	+4.390/ -4.720	26/ 27

In shaking table tests, specimens were successively excited by three earthquake records, such as El-Centro, Kobe or Chi-Chi TCU084, respectively. Fig. 8 shows the hysteretic response of largest intensity of acceleration in each test. In which, vertical axis of the force is calculated by the mass at top of the specimen multiplied by its acceleration, and the horizontal axis represents displacement measured at top of the specimens. Since the shear wall of the specimens has very large stiffness with not much weight of the mass at top of the specimen, all tests behaved in an elastic manner without any damage. For the two tests, it can be seen that the force and displacement at top of specimen with flange wall is far less than that of the specimens without flange wall. Tables 4 and 5 summarize the amplification rates of the acceleration measured at the top of mass related to the acceleration measured on the shaking table. Based on the stiffness and the mass at top of specimens, the calculating frequency for the specimens with or without the flange wall ranges as 6.4 Hz and 5.0 Hz, respectively. This amplification rates may be affected by the relation between the vibrating frequency of the specimen and the frequency content or composition in each exciting earthquake waves. For specimen with flange wall, the largest amplification rates is occurred by the excitation of TCU084, however, it is Kobe Earthquake for the specimen without flange wall due to the small difference in natural frequency exhibited in each specimen.

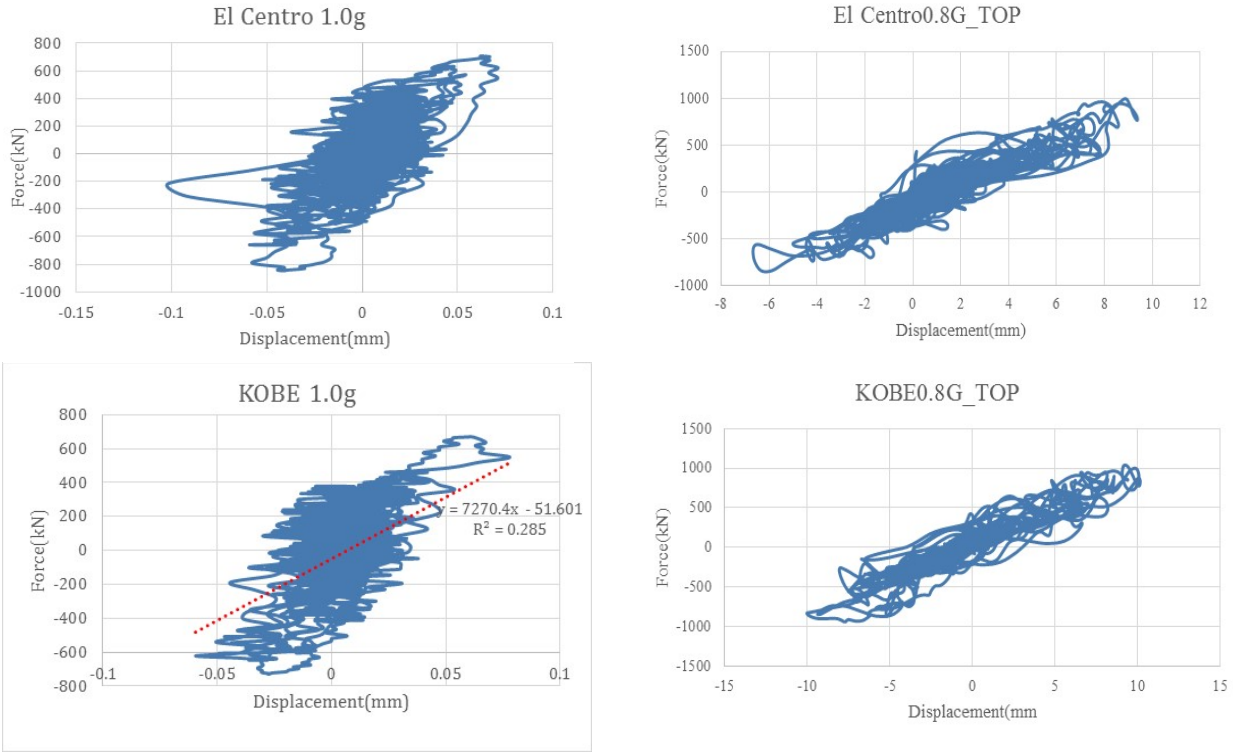

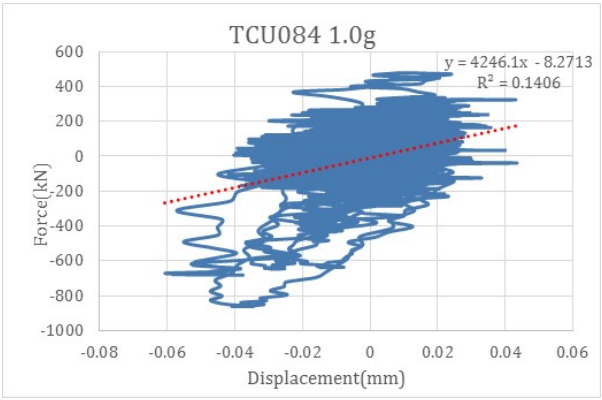

a) With Flange

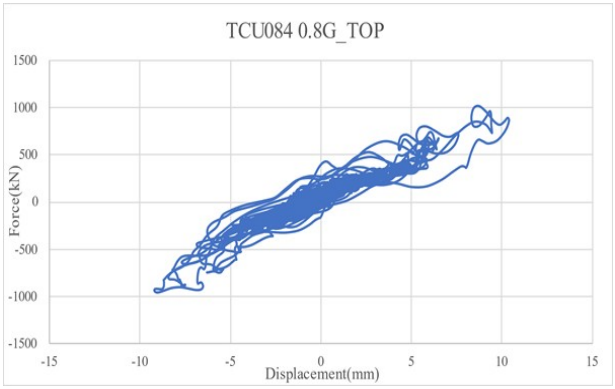

b) Without Flange

Fig. 8 Graphs show shaking table test response of two specimens.

Table 4 Amplification rates of specimens with flange at top of the mass

Earthquake	0.2g	0.4g	0.6g	0.8g	1.0g
El Centro	133%	122%	127%	140%	161%
Kobe	119%	114%	111%	110%	120%
TCU084	133%	143%	145%	140%	149%

Table 5 Amplification rates of specimens without flange at top of the mass

Earthquake	0.1g	0.3g	0.5g	0.6g	0.7g	0.8g
El Centro	148%	140%	133%	131%	106%	119%
Kobe	134%	141%	148%	200%	172%	198%
TCU084	153%	153%	140%	143%	154%	137%

CONCLUSION

This research investigated the seismic performance of low-yield steel and concrete composite shear walls subjected to in-plane shear and axial loads. Investigated parameters includes seismic effect of flange wall to the shear wall and strain rate of applying loads with static, high strain rate load and shaking table tests, respectively. Totally four specimens were constructed and six tests performed. Following is the summary of the test results.

1. All tests exhibited very good energy dissipation capacity with ultimate displacement ranged 3.8% to 7.5% for the shear wall.

2. There are 50 mm gap between the flange wall and top base plate so that axial load was applied on the shear wall only, and the presence of flange wall is acting as a lateral support for the shear wall in shaking table test. However, the flange wall increases 22% (630 kN) and 19% (560kN) of the peak strength under the static and high strain rate tests, respectively.

3. Peak shear strength in high strain rate dynamic tests had respectively 5% and 2.6% increase for the tests of the specimen with or without flange wall, when compared with its corresponding static tests. Similarly, the ultimate displacement of high strain rate dynamic tests for specimen with or without flange wall is averagely 2% and 0.7% more than that of corresponding static tests, respectively. As results, the dissipated energy in high strain rate dynamic tests is larger than that of its corresponding static tests.

4. In shaking table tests, specimens were excited by three earthquake records, such as El-Centro, Kobe or Chi-Chi TCU084, respectively. Since the shear wall of specimens has very large stiffness with not much weight of the mass at top of the specimen, all tests behaved in an elastic manner without any damage. The presence of the flange wall increased the lateral stiffness of the specimen, resluted in a small difference in natural frequency of the specimen. This may cause various seismic response for the specimen when excited by different earthquake waves due to its characteristic composition in frequency spectrum.

ACKNOWLEDGEMENTS

Donation of low-yield steels from China Steel Corporation is acknowledged. Financial support from National Science Council in Taiwan through grants MOST 109-2625-M-992-001 and 110-2625-M-992-002 is greatly appreciated. The authors would also like to thank Tainan Lab, National Center for Earthquake Engineering (NCREE) in Taiwan for the assistance in experiments.

REFERENCES

Chen, L., Mahmoud, H., Tong, S-M., and Y. Zhou (2015) "Seismic behavior of double steel plate–HSC composite walls," *Engineering Structures*, 102, pp.1-12.

Cheng, C-T., Y-C. Chang and H-Y. Chang (2019) "Cyclic in -plane shear performance of concrete-filled low-yield steel-plate composite walls in high-rise buildings," 21th Korea-Japan-Taiwan Joint Seminar on Earthquake Engineering for Building Structures (SEEBUS 2019), Dec. 6-7, 2019, Hsinchu, Taiwan, pp. 52-60.

Danay, A. (2012) "Response of steel-concrete composite panels to in-plane loading," *Nuclear Engineering and Design*, 242, pp. 52-62.

Epackachi, S., A.S. Whittaker, A.H. Varma, and E.G. Kurt (2015a) "Finite element modeling of steel-plate concrete composite wall piers," *Engineering Structures*, 100, pp.368-384.

Epackachi, S., A.S. Whittaker, and Y-N. Huang (2015b) "Analytical modeling of rectangular SC wall panels," *Journal of Constructional Steel Research*, 105, pp. 49-59.

Eom, T-S., H-G. Park, C-H. Lee, J-H. Kim, and I-H. Chang (2009) "Behavior of double skin composite wall subjected to in-plane cyclic loading," *Journal of Structural Engineering* (ASCE), 135(10), pp.1239-1249.

Fukumoto, T., B. Kato and K. Sato (1987) "Concrete filled steel bearing wall," IABSE Symposium, Paris-Versailles, 1987.

Hu, H-S., J-G. Nie, and M.R. Eatherton (2014) "Deformation capacity of concrete-filled steel plate composite shear walls," *Journal of Constructional Steel Research*, 103, pp.148-158.

Huang, Z., J.Y. Liew, Y.J. Richard, and J. Wang (2014) "Static behavior of curved lightweight steel-concrete –steel sandwich beams subjected to lateral loads." EUROSTEEL 2014, September 10-12, 2014, Naples, Italy.

Ji, X., X. Cheng, X. Jia, and A. H. Varma (2017) "Cyclic In-plane Shear Behavior of Double-skin Composite walls in High-Rise Buildings," *Journal of Structural Engineering* (ASCE), 143(6), 04017025.

Kurt, E. G., A.H. Varma, P. Booth, and A.S. Whittaker (2016) "In-Plane Behavior and Design of Rectangular SC Wall Piers without Boundary Elements," *Journal of Structural Engineering* (ASCE), 142(6), 04016026.

Lanning, J., G. Benzoni, and C.-M. Uang (2016) "Using buckling-restrained braces on long-span bridges. II: Feasibility and development of a near-fault loading protocol," *Journal of Bridge Engineering*, 21(5), 04016002.

Matsuishi, M. and S. Iwata (1987) "Strength of Composite System Ice-Resisting Structures Steel/Concrete Composite Structural Systems," C-FER Publication No. 1, Proceedings of a special symposium held in conjunction with POAC 1987, Fairbanks, Alaska, 9th International Conference on Port and Ocean Engineering under Arctic Conditions.

Nie, J-G., X-W. Ma, M-X. Tao, J-S. Fan, and F-M. Bu (2014) "Effective stiffness of composite shear wall with double plates and filled concrete," *Journal of Constructional Steel Research*, 99, pp.140-148.

Nie, J-G., H-S. Hu, J-S. Fan, M-X. Tao, S-Y. Li and F-J. Liu (2013) "Experimental study on seismic behavior of high-strength concrete filled double-steel-plate composite walls," *Journal of Constructional Steel Research*, 88, pp.206-219.

Ohno, F., T. Shioya, Y. Nagasawa, G. Matsumoto, T. Okada, and T. Ota (1987) "Experimental Studies on Composite Members for Arctic Offshore Structures Steel/Concrete Composite Structural Systems," C-FER Publication No. 1, Proceedings of a special symposium held in conjunction with POAC 1987, Fairbanks, Alaska,9th International Conference on Port and Ocean Engineering under Arctic Conditions.

Ozaki, M., S. Akita, H. Osuga, T. Nakayama, and N. Adachi (2004) "Study on steel plate reinforced concrete panels subjected to cyclic in-plane shear," *Nuclear Engineering and Design*, 228, pp. 225–244.

Rahai, A. and F. Hatami (2009) "Evaluation of composite shear wall behavior under cyclic loadings," *Journal of*

Constructional Steel Research, 65, pp.1528-1537.

Seo, J., A.H. Varma, K. Sener, and D. Ayhan (2016) “Steel-plate composite (SC) walls: In-plane shear behavior, database and design,” *Journal of Constructional Steel Research*, 119, pp. 202-215.

Varma, A. H., S.R. Malushte, K.C. Sener, and Z. Lai (2014) “Steel-plate composite (SC) walls for safety related nuclear facilities: Design for in-plane forces and out-of-plane moments,” *Nuclear Engineering and Design*, 269, pp. 240-249.

Vecchio, F. J., and I. McQuade (2011) “Towards improved modeling of steel-concrete composite wall elements,” *Nuclear Engineering and Design*, 241, pp.2629-2642.

Yan, J-B., and J.Y.R. Liew (2016) “Design and behavior of steel–concrete–steel sandwich plates subject to concentrated loads,” *Composite Structures*, 150, pp.139-152.

Zhang, K., A.H. Varma, S.R. Malushte, and S. Gallocher (2014) “Effect of shear connectors on local buckling and composite action in steel concrete composite walls,” *Nuclear Engineering and Design*, 269, pp. 231-239.

Zhao, W., Q. Guo, Z. Huang, L. Tan, J. Chen, and Y. Ye (2016) “Hysteretic model for steel–concrete composite shear walls subjected to in-plane cyclic loading, *Engineering Structures*, 106, pp.461-470.